TIMESCALE CONSIDERATIONS FOR INTERNAL COMBUSTION ENGINE SPRAYS

H. Lienemann and J.S. Shrimpton*
j.shrimpton@ic.ac.uk
***Imperial College of Science, Technology and Medicine**
Exhibition Road
London SW7 2BX, UK

Abstract

In this paper we address two issues related to direct injection spark ignition (DISI) engine operation. Firstly, we discuss the effects of ambient gas conditions on the characteristics of a spray produced by a pressure-swirl atomiser (PS-atomiser) and compare these to a dual fluid air-assisted atomiser (AA-atomiser) that has been tested under the same conditions in a constant volume chamber. Images from both sprays injected into gas densities characteristic of early, mid and late injection during the engine cycle have been post processed to extract penetration rate information for both sprays. Secondly, we use this data accompanied by data obtained with a Phase-Doppler-Anemometer (PDA) system to estimate drop momentum, heat up and evaporation timescales for both sprays as a function of drop diameter and in-cylinder conditions and relate these findings to engine timescales.

Introduction

In DISI engines as compared to port fuel injected (PFI) engines, there is a much greater emphasis on the mixture preparation stage because of the much shorter timescales involved for fuel atomisation, heat up, evaporation and air/fuel mixing in order to produce an ignitable mixture at the time of ignition. This applies in particular to DISI engines under stratified operation where fuel must be injected shortly before the time of ignition i.e. late in the compression stroke. One of the main problems related to injection and subsequent combustion in stratified operated DISI engines is high engine-out HC and NO_x emissions and soot emissions. It has been reported in previous studies on various DISI engine concepts that the mixture preparation time, the time from start of injection to ignition, is highly influential on these emissions [12, 13]. There are currently two principal ways of injecting fuel in DISI engines: single fluid, high-pressure injection and dual fluid, low-pressure injection. Single fluid injection systems operate at fuel pressures of between 50 and 120 bars with injection duration times in the range of 0.5 to 4.5 ms [1]. Single fluid PS-atomisers have been adopted by the engine industry [2, 3] due to their fine atomisation and wide spray dispersal. There have been a number of analytical [4, 5] and experimental [6] studies relating to the break-up of the liquid sheet whilst further experimental studies have focused on the spray characteristics [7, 8]. Dual fluid systems employ a sequenced pair of injectors in which air first pressurises a mixing chamber before the fuel-metering event begins. This two-phase charge resides for a short delay period before being injected into the combustion chamber. Air pressures of 6 to 10 bar and differential air/fuel pressures of ~1 bar are employed with charge injection duration times of 4 to 7 ms [1]. There have been a number of experimental and analytical studies [9, 10, 11] focusing on the operating parameters and spray characteristics of AA-atomizers and their application in DISI engines. The work described here focuses on the comparison of both systems in order to examine the performance of both injectors in DISI engines.

Experimental Set-up

The AA-atomiser is made of an assembly of a PFI fuel injector running at 9 bars and an air injector running at 7.5 bars absolute pressure. This is generally chosen as the best compromise between indicated fuel consumption and parasitic losses over the full engine speed/load range [9]. A compressed air bottle and two electrical fuel pumps provide the required air and fuel flow respectively. The constant volume chamber test rig (test conditions in table 1), the PS-atomiser test rig, the imaging system and the PDA system were exactly the same as previously described by Kashdan et al. [14]. In all tests, gasoline has been replaced by iso-octane (trimethyl-pentane 2,2,4) and the fuel delivery rate was 9.7 mg/injection for both injectors. Both injectors were found to have an inherent delay between the electrical start, defined by the rising edge of a TTL pulse and the emergence of liquid

P [bar]	T [K]	ρ [kg/m^3]	Injection strategy
1	300	1.3	'early'
5	300	5.8	'mid'
7	300	8.1	'late'

Table1. Chamber test conditions.

of approximately 0.27ms for the PS atomizer and 1.2 ms for the AA-atomiser. The electromechanical delay was found to vary slightly with P_{inj}, from 0.24ms at 20 bars to 0.27ms at 100 bars for the PS-atomiser [14] and 1.2ms at 1bar to 1.3ms at 5bar for the AA- atomiser. The injection pressure and injection duration were kept constant at 80 bars and 1.5ms for the PS-atomizer in all cases. For the AA injector the timings were fixed at 3.3ms for the fuel pulse width, 3.7ms for the air pulse width and 2.2ms for the fuel-air delay.

Comparison of Spray Characteristics

It was shown in previous experimental spray investigations [14, 15], that visualization studies reveal the spray to be axisymmetric on a macroscopic level and the images taken for this investigation have shown this to be the case for sprays from these particular injectors. Traversing the PDA radially across the spray performed a further verification of the spray symmetry. This allows us to regard one half of each image as representative for the whole spray image. Figure 1a-c show three split images (left: pressure-swirl, right: air-assisted) of both sprays taken 1.0ms aSOI injected into the pressurised chamber at pressures of 1 bar, 5 bars (double scale) and 7 bars (double scale). For interpretation of these pictures it should be noted that the PS-atomizer injects the same amount of fuel in a shorter period of time as compared to the AA-atomizer. It is clear from fig. 1 that both injectors produce a significantly different spray in terms of global shape and sensitivity to ambient pressure. The spray produced by the single fluid system is typical for a PS-atomizer, consisting of a characteristic 'pre-spray'

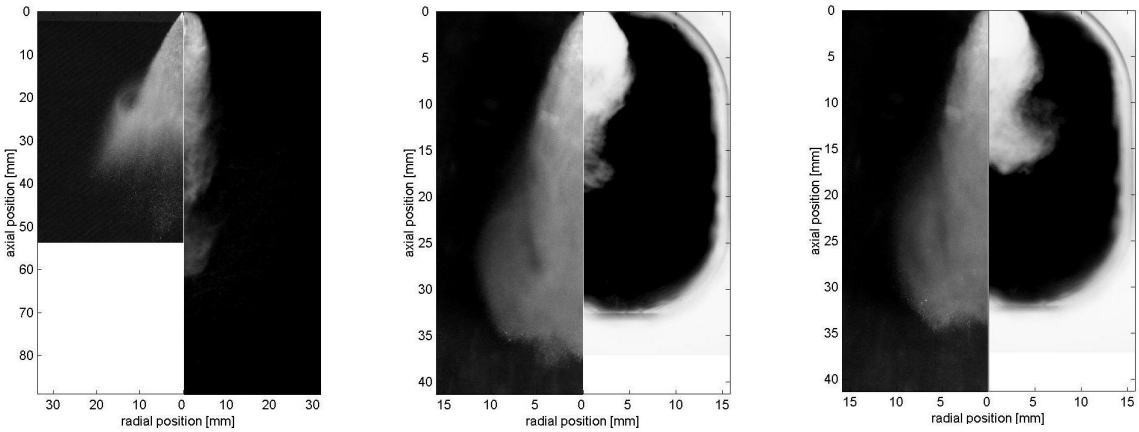

a b c

Figure 1. Spray images at 1.0 ms after hydraulic start of injection.

which is well ahead of the main spray with the main spray itself appearing as a cone which eventually widens up to form an 'umbrella' structure. This 'umbrella' shape is altered for increasing ambient pressures and becomes less obvious for the 5bars and 7bars chamber condition. In contrast the spray of the AA-atomiser appears in a shape more similar to a gas jet, about twice as long as the PS-atomiser and with a comparably high reduction in axial penetration as the ambient pressure increases.

A selection of sequential images was processed by means of edge detection algorithms to allow the spray development to be identified in terms of contour plots and penetration rate data. In contrast to the spray produced by the PS-atomiser a well-defined edge between ambient gas and the spray itself was detectable from images of the AA-atomiser spray showing no signs of a pre-spray. This is due to the different nature of the break-up mechanisms that the two different injectors make use of. The AA-atomiser produces droplets at low injection pressure predominantly through fuel droplet shearing [9] whereas the PS-atomizer relies on sufficient axial as well as radial momentum of the fuel at the head of the nozzle [14]. Penetration rate data for the PS-atomiser (Fig. 2a) reveal that the spray velocities in the near nozzle region were in the range of 50 to 70 m/s whilst PDA measurements have also confirmed this. The initial penetration rate for the AA-atomiser was found to be approximately 60 m/s for the atmospheric case (Fig. 2b). It then remains constant until about 1ms aSOI and 60mm from the nozzle exit before it follows a less than linear evolution. From fig. 1b,c it appears that the higher air density into which the fuel is injected has a marked effect in terms of suppressing both the axial and radial penetration for both sprays, which may be explained by means of the pressure difference across the atomiser nozzle. Given that the pressure difference represents the driving force behind the spray process, a reduction of the driving force of approximately 85% is noticeable for the AA-atomiser as the ambient pressure is increased from 1bar to 7bars compared to approximately 8% for the PS-atomiser. Therefore, it is clear from fig. 2a that the effect of increasing the chamber pressure from 1 to 5 bars reduces the spray penetration by approximately 25% at t=1.5ms aSOI for the PS-atomiser. However, further increasing ambient pressure from 5 to 7 bars was found to have relatively little effect. For the AA-atomiser the reduction of axial spray penetration is far more

significant. It is reduced by approximately 70% as the ambient pressure is increased from 1bar to 5bars at t=1.5ms (Fig. 2b). Whereas a significant reduction of the radial spreading rate is the most noticeable effect of the elevated chamber pressure on the pressure-swirl spray. For the atmospheric and 5 bar chamber conditions the measured cone angles were approximately 60° and 49° respectively. In case of the AA-atomiser the radial spray penetration rate was measured as the maximum spray width at any axial distance. It is evident from the spray images that the radial penetration decreases significantly for the upper and middle part of the spray for increasing ambient pressure. The spray width up to about 25mm downstream from the nozzle exit for time less than 1ms after hsoi decreases from approximately 20mm to 10mm, which is about the diameter of the injector poppet.

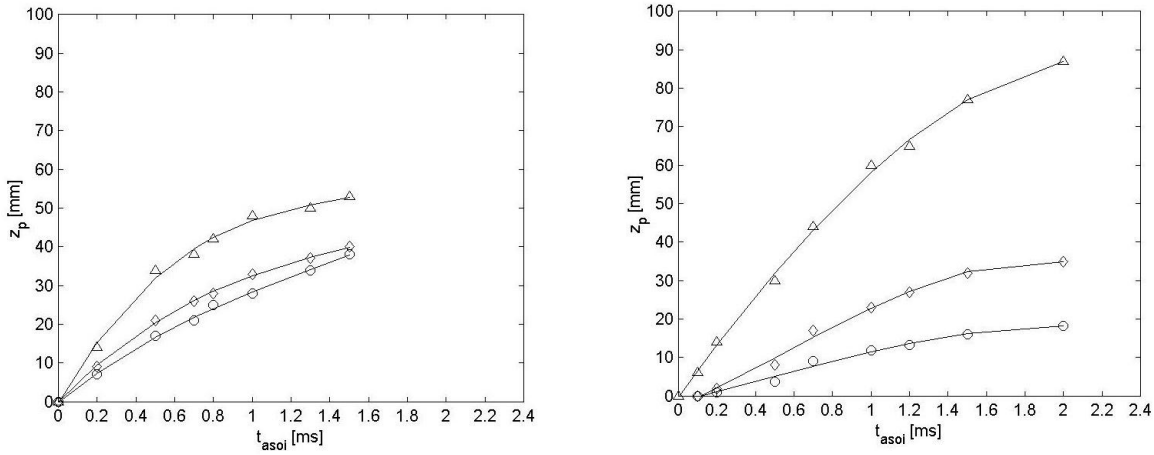

a b

Figure 2. Penetration rate data.

PDA results obtained on the injector centreline (R=0mm) at a downstream distance of 25mm from the nozzle exit for the PS-atomiser and 20mm from the nozzle exit of the AA-atomiser are presented in fig. 3a,b and 4a,b respectively for chamber pressures of 1, 5 and 7 bars. The discrete velocity and size data were processed into bins of 0.1 ms width. It is clear from fig. 3a that the chamber pressure has a significant effect on axial drop velocity as well as on drop sizes. In agreement with estimates made from spray tip penetration data for injection at atmospheric ambient pressure the velocity of the drops are high even at this downstream location with a peak of 0.75Uo, however the drops rapidly decelerate to ~0.32Uo by t=1.25ms aSOI (Fig. 3a). For Pch=7 bar the

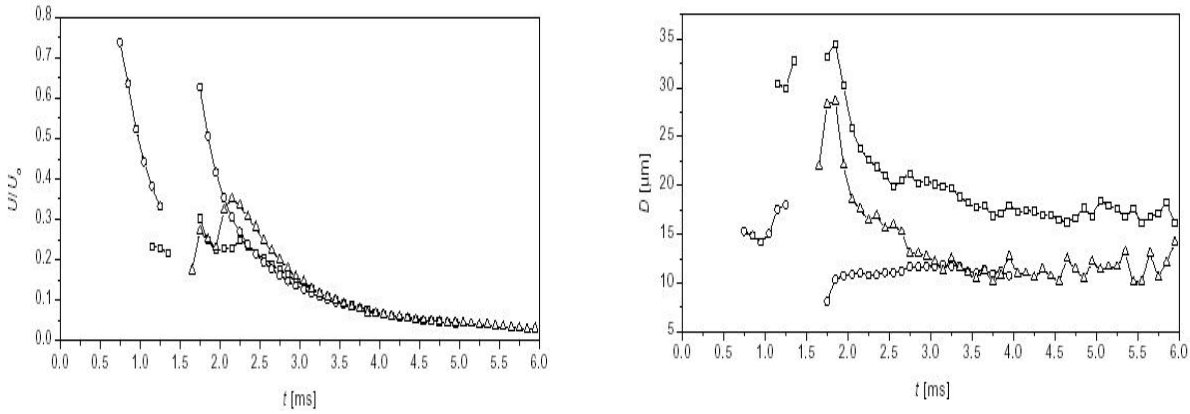

a b

Figure 3. PDA data for PS-atomiser.

higher air density causes a significant reduction in spray velocities. The initial drops have mean velocities of about 0.23Uo representing a 70% reduction when compared to the 1 bar case. For the time interval of 1.3<t<1.75ms aSOI attenuation of both the incident and scattered light caused by the dense spray cone makes valid measurements extremely difficult on the injector centreline as reported previously [18]. For t>1.75ms aSOI the trailing edge of the spray is measurable with velocities decreasing monotonically thereafter. The time evolution of the linear mean diameter is shown in fig. 3b. The drops measured within the pre-spray for Pch=1 bar are between 15-17 μm. In contrast, for Pch=7 bar the mean diameters at this location are significantly larger, between 30-33 μm for 1.1<t<1.3ms aSOI. The PDA data plots for the air-assisted spray (Fig. 4a,b) exhibit the

same lack of data as for the PS-atomiser for a time interval of approximately 4ms aSOI, which corresponds to the air pulse width of the injector (3.7ms). Thus the data in fig. 4a,b represent measurements in the trailing edge of the spray. However, captured data for 1bar and 5bars conditions reveal two similar characteristics as compared to the pressure-swirl spray. Firstly, a significant reduction of axial mean velocities as observed from the spray images. Secondly, an increase in the linear mean diameter (Fig. 4b). Droplets measured for the atmospheric case appear in a size range of 6 to 12 μm. In contrast, for Pch=5bars the mean diameter at the same location is significantly larger in a range between 12 and 22 μm. These findings have important implications for the adoption of atomisers for DISI engines. Whilst the atomisation performance may be sufficient for operation in the intake stroke with approximately ambient gas densities the challenge remains to employ later injection timings during the compression stroke thus exploiting part load fuel economy benefits. As discussed in the next section timescales for drop formation, transport and evaporation need to be short particularly at high engine speeds and for 'late' injection scenarios.

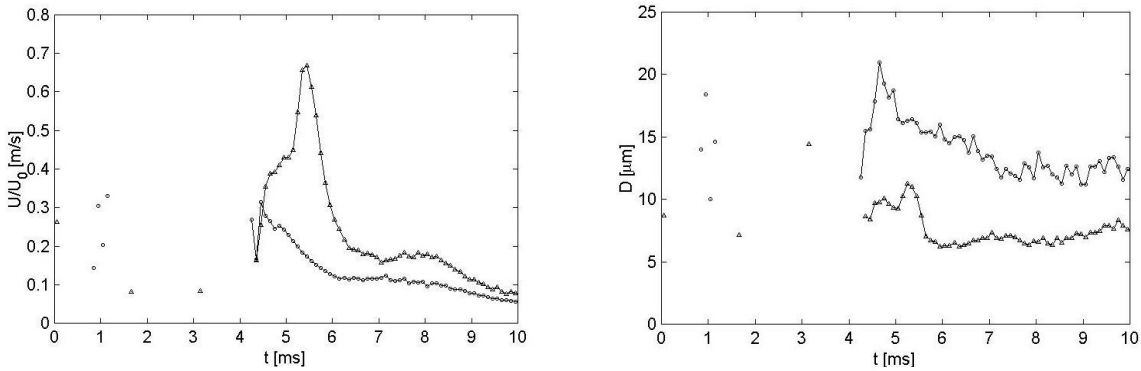

a b

Figure 4. PDA data for AA-atomiser.

Droplet versus engine timescales

The time required producing a combustible mixture of air and fuel vapour represents a significant fraction of the total time available for completion of combustion in internal combustion engines. Here we relate fuel drop evaporation time and drop deceleration time to the time available between injection and ignition in DISI engines by means of a single spherical drop of pure liquid having a well-defined boiling point [16]. The main equations and assumptions used are summarised in Table 2.

Main equations	Assumptions	Integrated equations
$m\frac{\delta u}{\delta t}=\frac{1}{2}\rho_g u_{rel}^2 \pi \frac{D^2}{4}C_D$ $C_D=\frac{24}{\mathrm{Re}}$ $C_D=\frac{24}{\mathrm{Re}}\left(1+\frac{3}{16}\mathrm{Re}\right)$	• Arithmetic mean of deceleration time from Oseen approximation and Stoke's law • U_0=70m/s(PS-atomiser) • U_0=60 to 12m/s(AA-atomiser, 1 to 5bar) • U_1=10m/s	$\Delta t_O=\frac{1}{b}\ln\left\|\frac{au}{au+b}\right\|_{u_1}^{u_0}, a=\frac{27\rho_g}{8\rho_d D}, b=\frac{18\mu_g}{\rho_d D^2}$ $\Delta t_S=\frac{D^2}{k}\ln\frac{u_0}{u_1}, k=18\frac{\mu_g}{\rho_d}$
$Nu=\frac{hD}{k_g}=2\frac{\ln(1+B_M)}{B_M}$ $\frac{dY_F}{dr}=-\frac{RT}{D_C P}(m_F Y_A)$	• Division of drop lifetime in heat up and steady state evaporation period (Lefebvre) • Quasi steady gas phase • Concentration gradient determines diffusion • Pure liquid	$\Delta t_{hu}=\frac{c_{pd}\rho_d c_{pg} D_{hu}^2 (T_{S_{st}}-T_{S_0})}{12k_g \ln(1+B_M)L(B_T/B_M-1)}$ $\lambda=\frac{8k_g \ln(1+B)}{c_{pg}\rho_d}$ $t_e=\Delta t_{hu}+\frac{D_1^2-D_e^2}{\lambda_{st}}$

Table 2. Summary of basic equations and assumptions.

Figure 5a,b illustrate the outcome of our calculation for the PS-atomizer and the AA-atomizer for different in-cylinder conditions together with typical engine timescales as described in section 1. Timescales for drop deceleration and engine operation are represented by the x-axis and corresponding drop sizes and engine speeds are shown on the y-axis. Each pair of the curves shown represent a different injection strategy. Figure 5a reveals that the limit for stratified operation is at about 3500 rpm for the PS-atomizer for late injection at 315° crank angle assuming a maximum drop size of 40 µm, which corresponds to the PDA measurements for 7 bar ambient

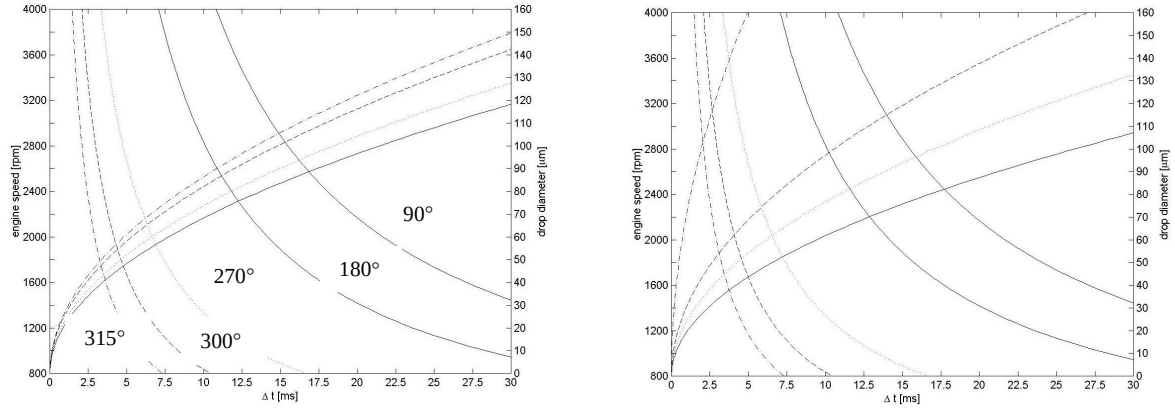

a b

Figure 5. Momentum decay timescales for PS- and AA-atomıser.

pressure presented in section 2. For these conditions the drop deceleration time as well as the engine timescale is the same at approximately 2 ms. If the drop size produced by the PS-atomiser was decreased to a maximum of 30 µm, the deceleration time would decrease to 1.5 ms and the range of stratified operation would increase to about 4500 rpm. The maximum drop size to be expected for injection at 300° crank angle according to PDA data presented in section 2 is 30 µm. This gives a deceleration time of about 2ms again, which is the same time available between injection and ignition for injection at 300° crank angle at about 4500 rpm and thus giving an extension of stratified operation to 4500 rpm. Injection at earlier points in the engine cycle such as 270° crank angle is less of a problem due to smaller drop sizes of about 20 µm and hence smaller deceleration times equal to about 1 ms and increasing time available between injection and ignition. For the AA-atomiser the curves representing the drop deceleration timescales are shifted towards smaller timescales compared to the PS-atomiser due to lower injection pressure. Drop sizes for the AA-atomiser range from 10 to about 20 µm. The combination of smaller drop sizes and smaller injection pressures lead to a much wider range of stratified operation.

Figure 6 illustrates the outcome of our calculation in the same manner as in Fig. 5 for the same in-cylinder conditions together with the same engine timescales. The first set of drop timescale curves corresponds to the time needed for a droplet of given diameter to heat up to ambient in-cylinder conditions. The second set of curves corresponds to the time needed for a drop to evaporate under these conditions. Under late injection conditions (315° crank angle) a typical drop of 35 µm diameter as produced by the PS-atomiser at these conditions needs about 3 ms to heat up and about 11 ms to heat up and evaporate. This time is considerably longer than the time available between injection and ignition, which ranges from approximately 8 ms at 800 rpm to 2 ms at 4000 rpm. The same problem arises for injection at 300° crank angle. A 30 µm drop formed at the nozzle of the PS-atomiser needs about 10 ms to heat up and evaporate, whereas the engine timescale reaches from 3 to about 10 ms. For 270° crank angle the corresponding times are 8 ms for the drop and 3 to 14 ms for the engine.

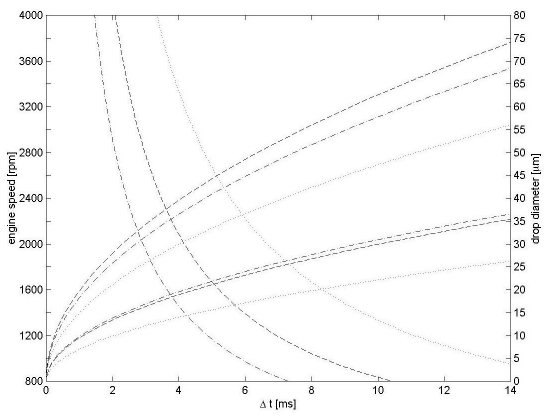

Figure 6. Evaporation and heat-up timescales.

Conclusion

It was shown that both injection systems produce drops of higher diameter for increased ambient gas densities. These findings were discussed in terms of engine timescales, which revealed that the mass transfer

timescale $\tau_m \propto D^2$ and thus the fuel drop diameter limit an overall homogeneous mixture preparation and therefore the speed range of stratified engine operation.

Nomenclature

m_F	fuel mass
D	drop diameter
D_{AB}	diffusion coefficient
μ	viscosity
ρ	density
λ_{st}	steady-state evaporation constant
B_M	mass transfer number
B_T	heat transfer number
T_{Sst}	drop steady state surface temperature
a,b,k	constants
Y_F	fuel ratio
Y_A	air ratio
t_e	drop lifetime
u_0	initial drop velocity
u_1	residual drop velocity
u_{rel}	relative drop velocity
C_D	drag coefficient
Re	Reynolds number
Nu	Nusselt number
T_{So}	drop initial surface temperature
k_g	thermal conductivity of fuel vapour
c_p	specific heat

Subscripts

g	gas
d	drop

References

[1] Wigley, G., "Initial comparison of single and dual fluid injectors for gasoline direct injection engines", ILASS-Europe 1999, Toulouse 5-7 July 1999.

[2] Y. Iwamoto, K. Noma, O. Nakayama, T. Yamauchi and H. Ando, "Development of Gasoline Direct Injection Engine", SAE Paper 970541, 1997.

[3] J. Harada, T. Tomita, H. Mizuno, Z. Mashiki and Y. Ito, "Development of Direct Injection Gasoline Engine", SAE Paper 970540, 1997.

[4] Z. Han, S. Parrish, P. V. Farrell and R. D. Reitz, "Modeling Atomization Processes of Pressure-Swirl Hollow-Cone Fuel Sprays", *Atomization and Sprays*, vol. 7, pp. 663-684, 1997.

[5] D. P. Schmidt, I. Nouar, P. K. Senecal, C. J. Rutland, J. K. Martin, R. D. Reitz and J. A. Hoffman, "Pressure-Swirl Atomization in the Near Field", SAE Paper, 1999-01-0496, 1999.

[6] T. Okamoto, T. Takagi, T. Kaji, K. Shimazaki and K. Nakanishi, "Studies on the Behaviour of Droplets and the Air Flow in a Hollow-Cone Spray", *Trans. of the ASME*, vol. 120, pp. 586-592, Sept. 1998.

[7] C. Jang, C. Bae and S. Choi, "Characterisation of Prototype High-Pressure Swirl Injector Nozzles, Part I: Prototype Development and Initial Characterisation of Sprays", *Atomization and Sprays*, vol. 10, no. 2, pp. 159-178, 2000.

[9] G. Cathcart, C. Zavier, "Fundamental characteristics of an air-assisted direct injection combustion system as applied to 4-stroke automotive gasoline engines", SAE Paper 2000-01-0256.

[10] G. Cathcart, D. Railton, "Improving robustness of spray guided direct injection combustion systems: the air-assisted approach", JSAE Paper 20015360.

[11] C. Jang, S. Kim, S. Choi, "An experimental and analytical study of the spray characteristics of an intermittend air-assisted fuel injector", *Atomization and Sprays*, vol. 10, pp.199-217, 2000.

[12] H. Sandquist, R. Lindgren, I. Denbratt, "Sources of hydrocarbon emissions from a direct injection stratified charge spark ignition engine", SAE Paper 2000-01-1906.

[13] H. Sandquist, I. Denbratt, A. Ingemarsson and J. Olsson, "Influence of fuel volatility on emission and combustion in a direct injection spark ignition engine", SAE Paper 982701.

[14] J. Kashdan, J. Shrimpton, C. Arcoumanis, "Pulsed fuel sprays for spray guided direct injection spark ignition engines: characterictic dynamics", *Atomization and Sprays*, accepted for publication.

[15] J. Kashdan**, "**Characteristics of pressure-swirl sprays", PhD Thesis, Imperial College, London 2002.

[16] A.Lefebvre, Atomization and Sprays, p.322, McGraw Hill, 1985.